Physicochemical Study of Eco-Friendly Sugar Palm Fiber Thermoplastic Polyurethane Composites

Ausama A. Mohammed,[a,b,*] Dandi Bachtiar,[a] Januar P. Siregar,[a] Mohd. R. M. Rejab,[a] and Syed F. Hasany [c]

The physicochemical properties of an innovative and environmentally friendly composite material based on sugar palm fiber (SPF) and thermoplastic polyurethane (TPU) were examined. The base material with short fibers was extruded and hot pressed to produce the TPU-SPF composites with different synthetic parameters. Operating parameters including temperature for extrusion (170 to 190 °C), rotational velocity (30 to 50 rpm), and fiber particle sizes (160, 250, and 425 µm) were investigated. The aims were to optimize rotational velocity, temperature, and fiber size of the TPU-SPF composites. Firstly, the influence of rotation of velocity and temperature on the tensile properties was investigated. Secondly, effects of different fiber sizes on tensile, flexural properties, and impact strength as per ASTM standards were tested. The morphological, thermal, and physicochemical properties of the synthesized TPU-SPF composites were ascertained with Fourier transform infrared spectroscopy (FT-IR), scanning electron microscopy (SEM), X-ray diffraction (XRD), and thermogravimetric analysis (TGA). The optimal results were observed with a temperature of 190°C and a rotational velocity of 40 rpm. Meanwhile, the strength and modulus for tensile and flexural were best for fiber size 250 µm. Moreover, the impact strength reached a peaking trend at 250 µm fiber size.

Keywords: Environmentally friendly composites; Thermoplastic polyurethane; Sugar palm fiber

Contact information: a: Structural Materials and Degradation Focus Group, Faculty of Mechanical Engineering, University of Malaysia Pahang, 26600, Pahang Darul Makmur, Malaysia; b: Department of Materials Engineering, University of Technology, Baghdad, Iraq; c: Faculty of Chemical and Natural Resources Engineering, University of Malaysia Pahang, 26600, Pahang Darul Makmur, Malaysia;
** Corresponding author: phd_78@yahoo.com*

INTRODUCTION

Natural fiber-reinforced polymers are gaining more attention over synthetic fibers in composites (Dittenber and GangaRao 2012), due to better results in the abrasiveness of the equipment, cost reduction, renewability, biodegradability, and good mechanical strength (Biagiotti *et al.* 2004; Pilla 2011). Natural fibers such as flax (Bos *et al.* 2006), wood (Ratnam *et al.* 2010), hemp (Wötzel *et al.* 1999), waste cellulosic products (Jawaid and Khalil 2011), and jute (Roy *et al.* 2012) have been studied intensively as alternatives to synthetic fibers. The petroleum thermoplastic polyurethanes (TPU) are greatly needed in many industries, as they are used in the automotive instrument panels (Engels *et al.* 2013), sporting goods, caster wheels, medical devices, power tools, drive belts, inflatable rafts, outer cases of mobile electronic devices, and footwear (Herrera *et al.* 2002). The TPU has unique properties due to the inter-molecular interactions and a distinctive combination

of molecular mobilities that contribute to high toughness, durability, tensile strength, and tear resistance and wear when composited with the natural fiber (Gunatillake *et al.* 2006).

Lack of compatibility is one of the problems facing natural fiber polymer composites. The hydrophobic nature of most polymers used in this field versus the hydrophilicity of natural fibers causes poor adhesion and wettability. However, one of the hydrophilic polymers is polyurethane, which would not face this kind of incompatibility (Özgür and Oksman 2008). Kenaf fiber composites with TPUs show significant changes in the tensile properties depending on the fiber loading in the TPU matrix (El-Shekeil *et al.* 2011; El-Shekeil *et al.* 2012a,b). Cocoa (*Theobroma cacao*) pod husk fiber-reinforced TPU has an increased modulus and tensile strength with increases in the fiber content and decreases in strain (El-Shekeil *et al.* 2014). The development of new composites needs optimal parameters, such as time, speed, and temperature, for the best outcomes (Vera-Sorroche *et al.* 2013). Due to their higher cost of production and less environmentally friendly approach, researchers are keen to find alternatives such as green/natural composites that fulfill the industrial requirement of cost reduction, renewability, and biodegradability (Pilla 2011).

The development of eco-friendly sugar palm fiber thermoplastic polyurethane composites using an extruder needs proper settings for parameters such as speed and temperature in order to get the best results. The processing speed might lead to the breakage of the fibers if high speed is applied. On the other hand, low speed is inadequate to mix the compounds well. This may lead to the non-homogeneous distribution of fibers in the matrix. Moreover, the temperature is critical in processing; if it is high, thermal degradation of the fibers as well as the matrix may take place.

Sugar palm fibers (SPF) are widely employed in septic tanks for filtration, distilled water filtration, chair cushions, brooms, door mats, brushes, roofs, carpets, fish nets, and ropes (Bachtiar *et al.* 2010) due to their high durability, reproducibility, and wear resistance in a composite matrix (Ishak *et al.* 2013). SPF has limited applications in polymer composites, except with some epoxies (Bachtiar *et al.* 2008, 2009; Sapuan and Bachtiar, 2010) and high impact polystyrene (Bachtiar *et al.* 2011, 2012). However, the role of the SPFs as reinforcements in the thermoplastic composites with TPU has not been studied.

This study developed and optimized the TPU-SPF composites at 90/10 by wt.%. The effect of different rotation speeds (30, 40, 50 rpm) and temperatures (transition phase temperature) (170, 180, 190 °C) on the tensile properties and different fiber sizes (160, 250, 425 µm) on the mechanical properties (tensile, flexural, and impact) of the composites were investigated. The composite surfaces were characterized by the Fourier transform infrared (FT-IR), X-ray diffraction (XRD), and scanning electron microscopy (SEM), spectroscopy. The thermogravimetric analysis (TGA) was conducted to evaluate the thermal stability of the composite.

EXPERIMENTAL

Materials

Polyether-type thermoplastic polyurethane (specific gravity of 1.13) was used as supplied by Bayer Co. (Malaysia) Sdn Bhd (Petaling Jaya, Selangor, Malaysia). The sugar palm fiber (SPF) was collected locally from Raub, Pahang, Malaysia.

Fiber Preparation

The SPFs were washed, dried at 35 °C for 14 days, mechanically cut into 1-cm pieces, and crushed by a grinder (Retsch Ultra Centrifugal Mill Model ZM200, Haan, Germany). The particles were separated by three different sieves to get the desired fiber sizes of 160, 250, and 425 µm by a Fritsch Analysette 3 auto shaker (Idar-oberstein, Germany).

Preparation of Composites

All the TPU-SPF composite specimens were compounded by using a ThermoScientific Eurolab 16 extruder machine (Karlsruhe, Germany). A 10% fiber loading was fixed throughout this study. The samples were prepared at different processing parameters such as speed (30, 40, and 50 rpm), temperatures (transition phase) (170, 180, and 190 ºC) and fiber sizes (160, 250, and 425 µm). Table 1 shows the experimental study procedure for different processing parameters to find the best tensile strength of the TPU-SPF composites. Mechanical results are discussed in detail in result and discussion.

Table 1. Experimental Steps to Study the Different Processing Parameters for the TPU-SPF Composites at 10% wt. Fiber Loading

Steps	First parameter speed (rpm)	Second parameter temperature (°C)	Third parameter fiber size (µm)	Tensile strength (MPa) (current study)	Note
1st	30 40 50	190 180 170	160 250 425	--	Selected range of every parameter
2nd	30	190	250	7.344	Temperature and fiber size were fixed; Speed was varied
	40	190	250	10.62	
	50	190	250	7.144	
3rd	--	--	--	10.62	The highest value of tensile strength for different rotation speed was witnessed at 40 rpm, 190 °C, and 250 µm
4th	40	190	250	14.01	Speed and fiber size were fixed; Temperature was varied
	40	180	250	7.19	
	40	170	250	9.054	
5th	--	--	--	14.01	The highest value of tensile strength for different temperature was witnessed at 190 °C, 40 rpm, and 250 µm
6th	40	190	160	12.84	The optimum speed and temperature were fixed, with different fiber size
	40	190	250	14.01	
	40	190	425	7.9	
7th	--	--	--	14.01	The highest value of tensile strength for different fiber size was witnessed at 250 µm, 40 rpm, and 190 °C
8th	40	190	250	14.01	These are the experimental results which recorded the best tensile strength

Initially, the low-temperature compounding (LTC) with the extruder temperature set at 200 °C (near the melting temperature of TPU) was performed. The addition of SPF in the TPU resulted in an increase in the viscosity of the mixture, which may have degraded the fiber due to an increase in the melting temperature and torque load; to control the degradation, the temperature ranged from 170 °C to 190 °C in the "transition phase" during different temperature studies. In the "steady-state phase", the temperature was also varied between 160 °C and 180 °C in different temperature studding (Caulfield *et al.* 2001; Misra *et al.* 2004). Fibers of different sizes (160, 250, and 425 µm) were studied to find the best tensile strength. The extruded composite pellets were later pressed with a Lotus Scientific 25-ton compression molding machine (Shah Alam, Malaysia) for 10 min at 190 °C. The molds were prepared with dimensions of 200 × 200 × 3 mm for length, width, and thickness, respectively.

Characterization of Composites

Tensile testing

An Instron universal testing machine model 3369 (Norwood, USA) with a crosshead velocity of 5 mm/min was used for calculating the tensile properties. Five specimens were cut into dumbbell shapes according to ASTM D638-02a (year 2002), as shown in Fig. 1(a).

Flexural testing

The flexural testing was performed on the same Instron universal testing machine with three points bending and a crosshead velocity of 2 mm/min. The span length was equal 16 times of the specimen thickness; it means 48 mm according to ASTM D790. The sample dimensions were 130 × 13 × 3 mm according to ASTM D790 (1974) as shown in Fig. 1(b).

Impact testing

The samples for the notched impact strength testing were prepared per ASTM standard D256 (1996), with dimensions of 63 × 13 × 3 mm (Fig. 1(c)). The samples were tested on a Zwick/Roell 5113 pendulum impact machine (Ulm, Germany). The impact strength (kJ/m^2) was evaluated by dividing the impact energy from the cross-section area in all samples.

Morphological and chemical analysis

Fourier transform Infrared spectroscopy (FT-IR) was recorded on the (ThermoScientific iS50 FT-IR, Madison, USA) scanning from 525.0 to 3994.5 cm^{-1}. About 2 mg of SPF was crushed to small particles. The fiber particles were pressed into small discs about1-mm thickness. X-ray diffraction (X-RD) (Rigacu model Mini Flex, Japan). XRD studies were carried out under ambient conditions using Cu Kα (1.5418 °A) radiation, a Ni-filter, and a scintillation counter as a detector at 30 KV and 15 mA on rotation between 3^o to 70^o at 2θ scale at 1-second step size and increments of 0.02 degree with 0.5^o or 1.0 mm of divergent and anti-scattering slits. The scanning electron microscopy (SEM) (Carl Zeiss model EVO, Germany) was employed to study the morphology of the polymer complexes. The samples were fixed on aluminum sample holders with a carbon tape and coated with platinum to a thickness of approximately 250 °A. The experimental conditions for all samples were: 6.5 to 11 mm working distance (WD), 5-20 kV (EHT) accelerating

voltage, and high vacuum. Finally, the thermal gravimetric analysis (TGA) (Mettler Toledo, Swiss) was employed for chemical and thermal examination of the prepared samples. The tests were carried out in an atmosphere of nitrogen flowing, and the heating rate of 10 mL/min, 10 °C/min respectively, with temperature range between the room temperature and 600 °C. Every sample between 4 and 10 mg of the materials was heated in a small crucible.

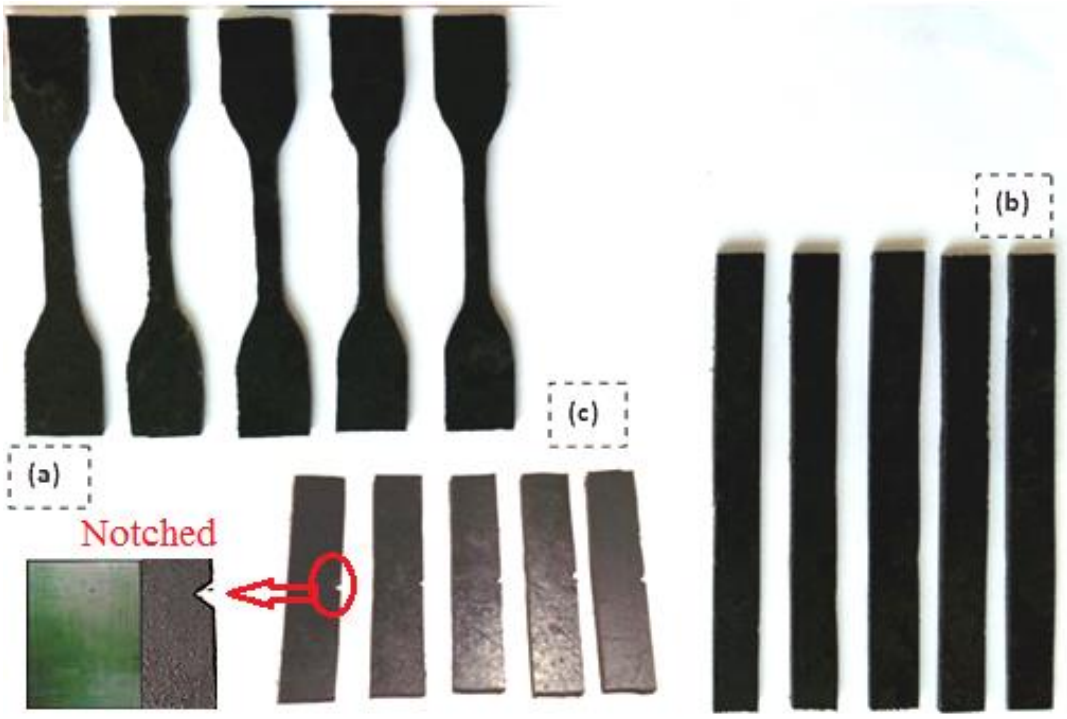

Fig. 1. (a) Tensile specimens, (b) flexural specimens, and (c) impact specimens

RESULTS AND DISCUSSION

Process Optimizing Parameters and Mechanical study

The process optimizing parameters (rotation velocity, the temperature of extrusion reaction, and fiber particle size) were studied in developing new TPU-SPF composites.

Effect of change in rotational velocity

Figure 2 shows the effects of rotational velocity on the tensile strength of the TPU-SPF composites at a fixed temperature ranges (180, 190, and 200 °C), and fiber size 250 µm, respectively. Three different rotation velocities; 30, 40, and 50 rpm were examined. The tensile strength increased from 7.344 MPa to 10.62 MPa when the rotational velocity was increased from 30 to 40 rpm, while the tensile strength declined to 7.144 MPa at 50 rpm, which may reflect the large friction and fiber breakage.

The reduction of strength of the increasing speed was most probably due to the friction and breakage of the fibers. On the other hand, at lower speeds the materials were not homogeneous. However, there were slightly decreased strain values from 30.7% at 30

rpm to 30.37% at 40 rpm and 29.9% at 50 rpm. The modulus decreased from 48 MPa to 22 MPa at 30 rpm and 40 rpm, respectively, but increased at 50 rpm to 76 MPa, which showed a good dispersion of fiber in the polymer matrix (Kanimozhi *et al.* 2014). The maximum tensile strength was 10.62 MPa observed at the rotational velocity of 40 rpm, as reported previously (El-Shekeil *et al.* 2011); therefore, it was taken as the optimum velocity in further synthesis reactions.

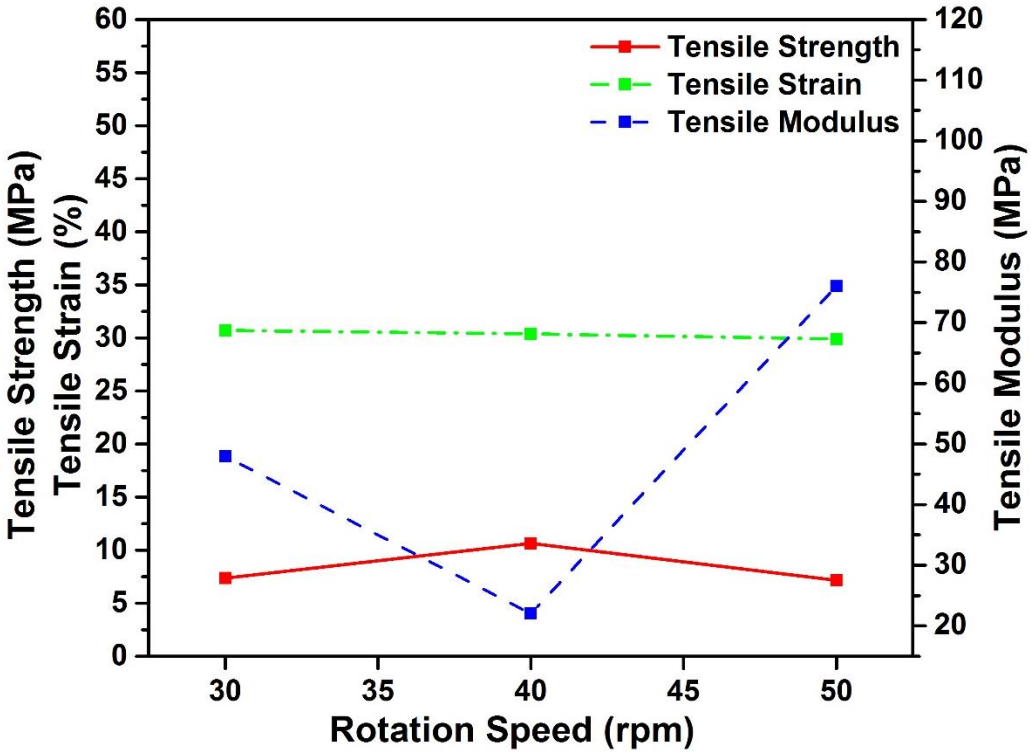

Fig. 2. Effects of the setting velocity on the tensile strength, modulus, and strain of TPU-SPF composites

Effects of change in the operating temperatures

Figure 3 depicts how changes in temperatures (transition) affected the tensile strength of TPU-SPF composites at optimum rotational velocity (40 rpm). The temperature values were maintained at 170, 180, and 190 °C with a fiber size of 250 µm. The starting temperature was maintained at 200 °C to avoid the melting TPU and degrading the SPF.

The tensile strength decreased from 170 to 180 °C (9.054 to 7.19 MPa) but increased markedly at 190 °C (14.01 MPa). The higher strength value at 190 °C indicates better interfacial bonding compared with the other two temperatures. Thus, 190 °C was taken as the optimized transition zone temperature. Strain values rapidly decreased from 170°C (75%) to 180 °C (34%), while a slight increase was observed at 190°C (39%). The modulus increased from 170 °C (46 MPa) to 180 °C (57 MPa) but decreased at 190 °C (23 MPa), which suggested a good distribution of SPF in the TPU (Liang and Li 1998; Liang *et al.* 1999; Liang 2012).

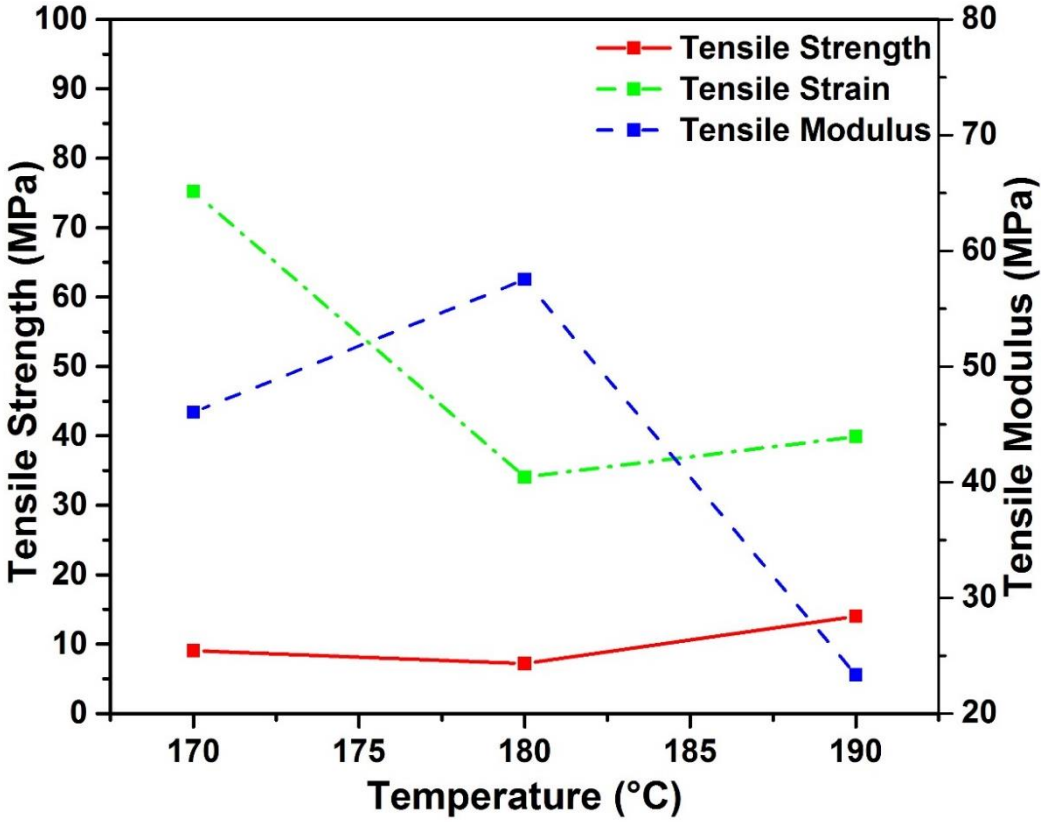

Fig. 3. Effects of setting temperature (transition phase) on the tensile properties of the TPU-SPF composites

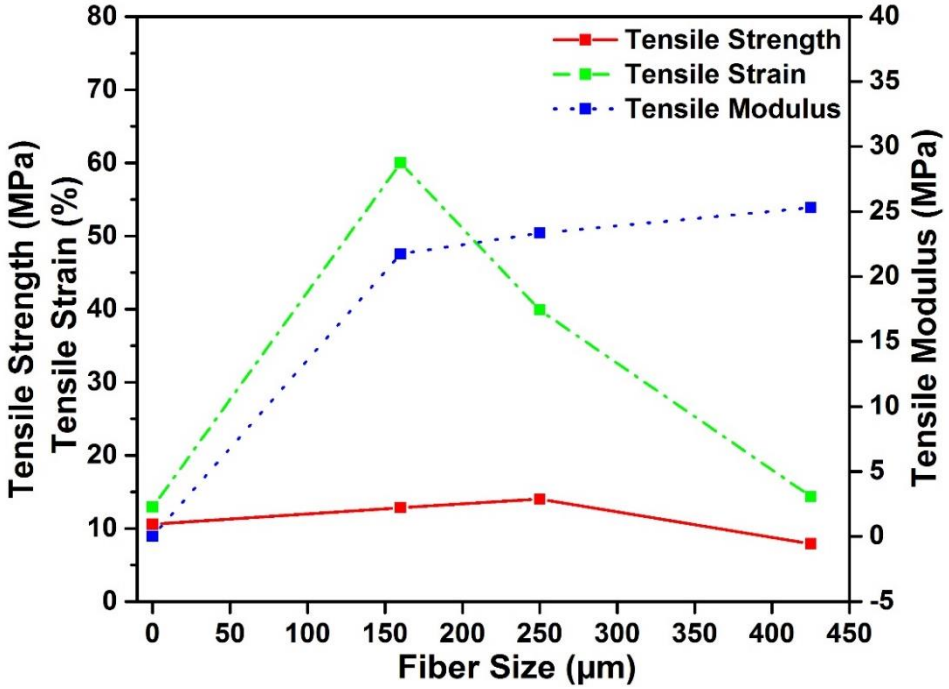

Fig. 4. Effects of the fiber size on the tensile strength, modulus, and strain of TPU-SPF composites

Effects of change in fiber size

The effects of fiber size on the tensile properties of the TPU-SPF composites were studied at the optimum rotational velocity (40 rpm) and temperature (190 °C) with three different SPF fiber sizes (160, 250, and 425 µm) (Fig. 4). The strength values increased from 12.84 MPa (160 µm) to 14.01 MPa (250 µm) but were reduced to 7.9 MPa for the fiber size of 425 µm. In contrast, the strain values were lowered at 160 µm (60%), 250 µm (40%), and at 425 µm (14%), respectively. The modulus increased slightly with the increasing fiber size (22 MPa, 23 MPa, and 25 MPa for 160 µm, 250 µm, and 425 µm, respectively) (Verhoeven 2006; El-Shekeil *et al.* 2011).

Taking all results together, the optimized tensile strength value (14.01 MPa) of the TPU-SPF composites was observed at a velocity of 40 rpm, temperature of 190 °C, and fiber size of 250 µm. The composite optimum tensile strength was higher than the tensile strength of pure TPU which was 11 MPa.

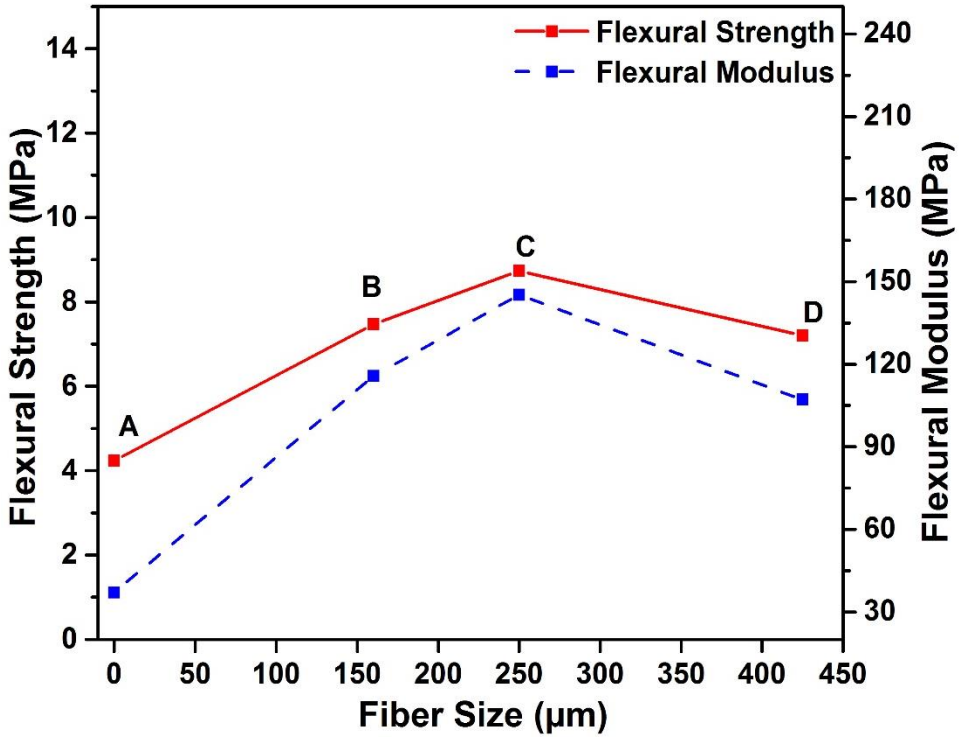

Fig. 5. Effects of the fiber size on flexural properties. (A) TPU; (B, C, and D) TPU-SPF composites

Flexural strength and flexural modulus

Figure 5 shows how the flexural strength of the TPU and TPU-SPF composites was influenced by the fiber size at the optimum rotation velocity of 40 rpm at a temperature of 190°C. The flexural strength and modulus of the pure TPU were recorded as 4.234 and 37.108 MPa, respectively. The flexural strength increased from 7.47 MPa in the TPU-SPF with 160 µm fiber to 8.735 MPa in the TPU-SPF with 250 µm fiber. The flexural strength in the TPU-SPF with 425 µm decreased to 7.199 MPa. The modulus displayed the same trend, increasing from 115.7 MPa to 145.3 MPa and then decreasing to 107.1 MPa in the

TPU-SPF with 160 µm, 250 µm, and 425 µm fibers, respectively. The same trend was observed previously in the kenaf/TPU composites (El-Shekeil *et al.* 2011; Kim *et al.* 2013).

Impact strength study at different fiber sizes

The impact strength of the TPU-SPF composites was studied with different fiber sizes of SPF (160, 250, and 425 µm) with optimum rotation velocity 40 rpm, at a temperature of 190 °C. The impact strength observed was 92.93, 71.67, 100.2, and 72.7 kJ/m^2 for 160 µm TPU-SPF, 250 µm TPU-SPF, and 425 µm TPU-SPF respectively. The highest impact strength value was recorded the highest value with a fiber size of 250 µm (Fig. 6). This result indicates that increasing fiber size has a positive effect on the impact strength up to certain size; after that point, the increased fiber size decreased the impact strength because of problems in dispersion and larger agglomeration (Matheson 2009).

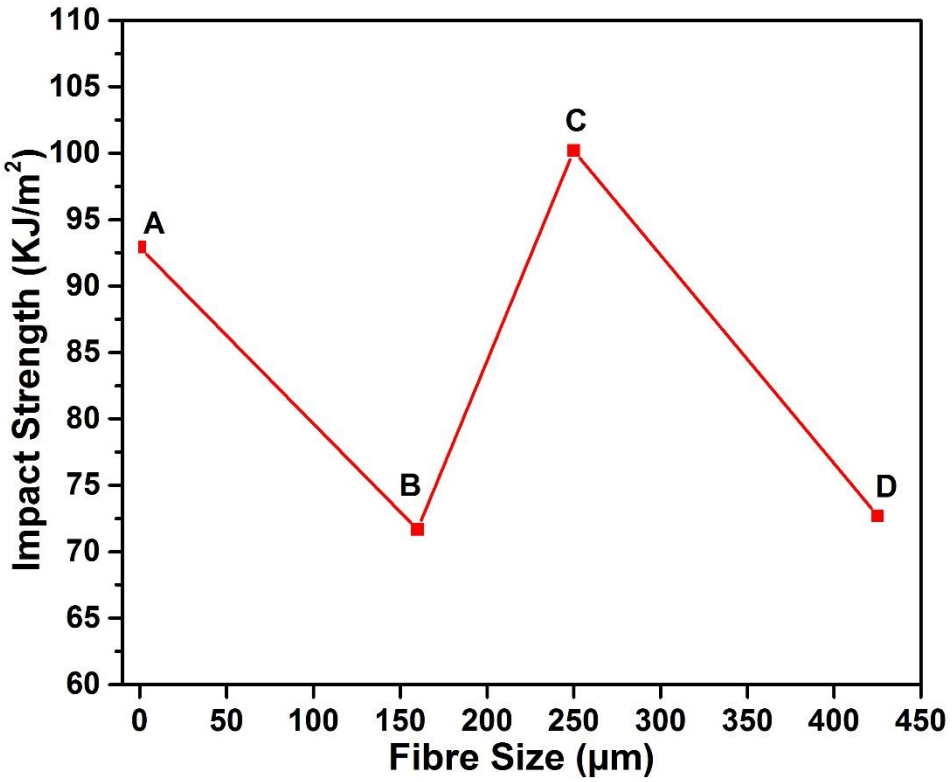

Fig. 6. Effects of the fiber size on the impact strength; (A) TPU; (B, C, and D) TPU-SPF composites

Chemical and Morphological Analysis

FT-IR studies

Figure 7 depicts the FT-IR spectra of the neat TPU and different sizes of the sugar palm fiber (SPF), reinforced with the TPU system, which showed identical behavior just like the neat TPU, *i.e.* identical peaks but with low intensity (Kanimozhi *et al.* 2014). This result was attributed to the fact that the untreated fiber is grafted on the polymer surface by physical interactions such as hydrogen bonding which resulted in the low-intensity C=O peaks.

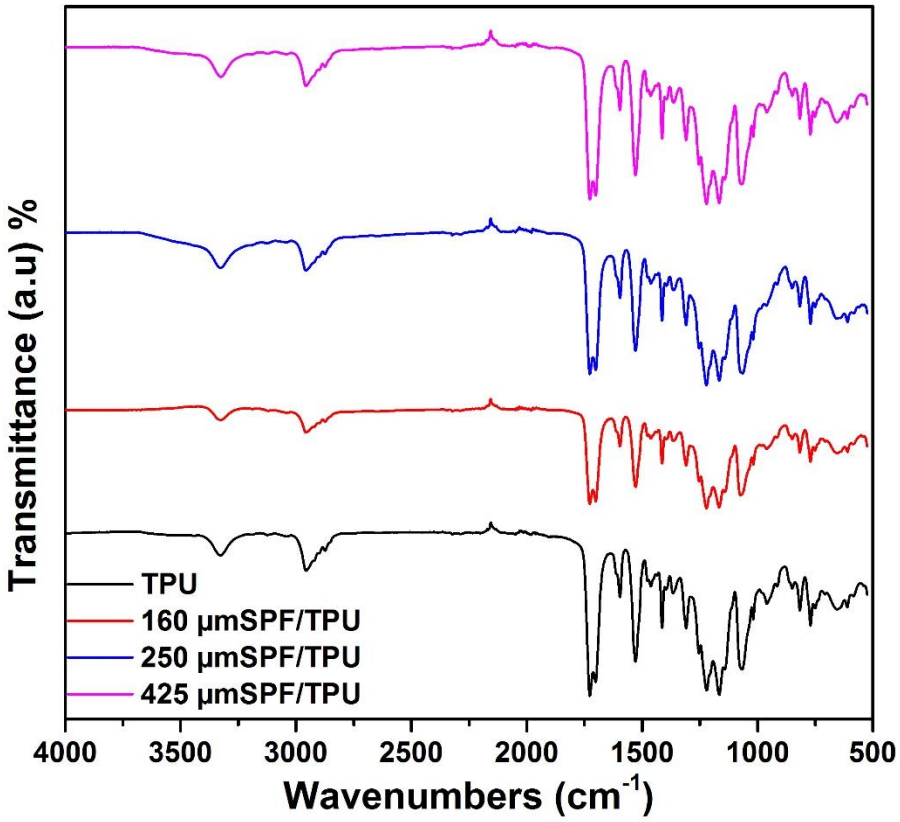

Fig. 7. FTIR of pure TPU and TPU-SPF composites

Table 2. Main FTIR Bands of Pure TPU, and 160 µm TPU-SPF, 250 µm TPU-SPF, 425 µm TPU-SPF Composites

Peak Location (cm^{-1})	Chemical Structure	Motion	Pure TPU	TPU-SPF 160 µm	TPU-SPF 250 µm	TPU-SPF 425 µm
3,420 - 3,200	N–H	Stretching	3326.22	3328.04	3327.02	3325.32
1,590 - 1,650	N–H	Bending	1596.29	1596. 10	1596.21	1596.25
3,000 - 2,800	CH_2 and CH_3	Stretching	2956.55	2956.71	2956.85	2956.84
1,740	C=O	Non-bonded urethane Stretching	1726.92	1727.22	1727.90	1726.57
1,690	C=O	Associated urethane	1701.12	1701.09	1701.02	1701.25
1,550 - 1,510	H–N–CO	Combined motion	1529.27	1528.74	1529.20	1529.22

The 160 µm fiber showed much lower intensities than 250 and 425 µm samples, which may be due to a high value of adherence on the polymer surface. The hydrogen bonding between TPU and the untreated TPU-SPF in different sizes caused a minimal

increase in the transmittance frequency of C=O group (Table 2). The virgin TPU C=O was absorbed in 1726.92 cm^{-1} while the TPU-SPF of sizes 160, 250, and 425 µm showed 1727.22, 1727.9, and 1726.57, respectively.

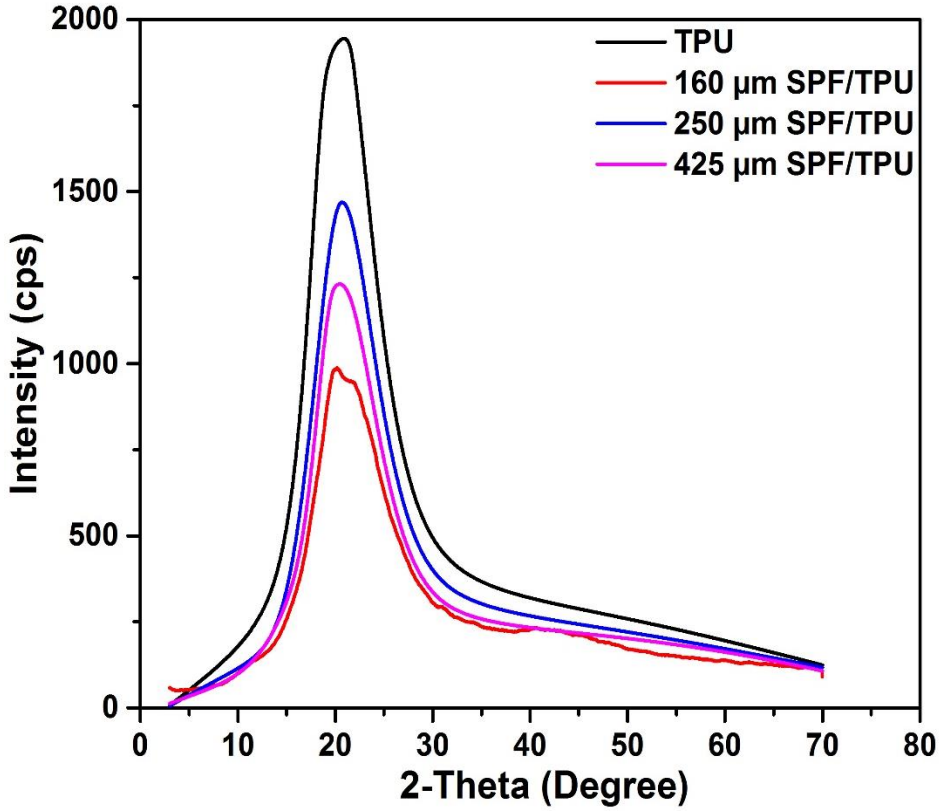

Fig. 8. XRD of pure TPU and TPU-SPF composites

X-ray diffraction

XRD analysis was used to investigate the different short fiber size of SPF 160, 250, and 425 µm, and reinforced TPU composites. The diffractograms are presented in Fig. 8. There was no diffraction peak observed for TPU composites. The absence of the diffraction peak in reinforced composites is due to the complete exfoliation of the different SPF into the TPU network structure. The observance of peak at 2θ = 23° showed the amorphous nature, and the uniform level dispersion of SPF concurrently confirmed the efficient and effective compatibility between the SPF and the TPU matrix. Except the fiber size 250 µm, the reading was with less intensity. SPF dispersion was homogenously observed in the form of individual layers within the polymer matrix, and leading to exfoliated composites with improved properties (Kanimozhi *et al.* 2014).

SEM analysis

Figures 9a and b shows the SEM images of the pure TPU, SPF fiber, and TPU-SPF with fiber size 160 µm (Fig. 9c), 250 µm (Fig. 9d), and 425 µm (Fig. 9e) composites. The pure TPU had a smooth glassy fractured surface at different places (Fig. 9a). Moreover, the TPU-SPF composites showed poor fiber-matrix adhesion, as gaps were observed between

the fibers the matrix, and the fibers were easily pulled out. The fiber sizes of 160 and 425 µm in Fig. 8c and e had negative effects on the fiber-matrix adhesion, resulting in low mechanical properties in these composites perhaps due to the surface of fiber with more impurities (untreated fiber). However, the composite with 250 µm fiber showed the best adhesion with the TPU matrix in Fig. 9d. This result may be due to the suitable surface area for the 250 µm fiber size to the adhesion with the TPU matrix, which provides the appropriate opportunities to increase the interfacial adhesion and form a uniform surface with a higher mechanical strength (Aji *et al.* 2011; El-Shekeil *et al.* 2011).

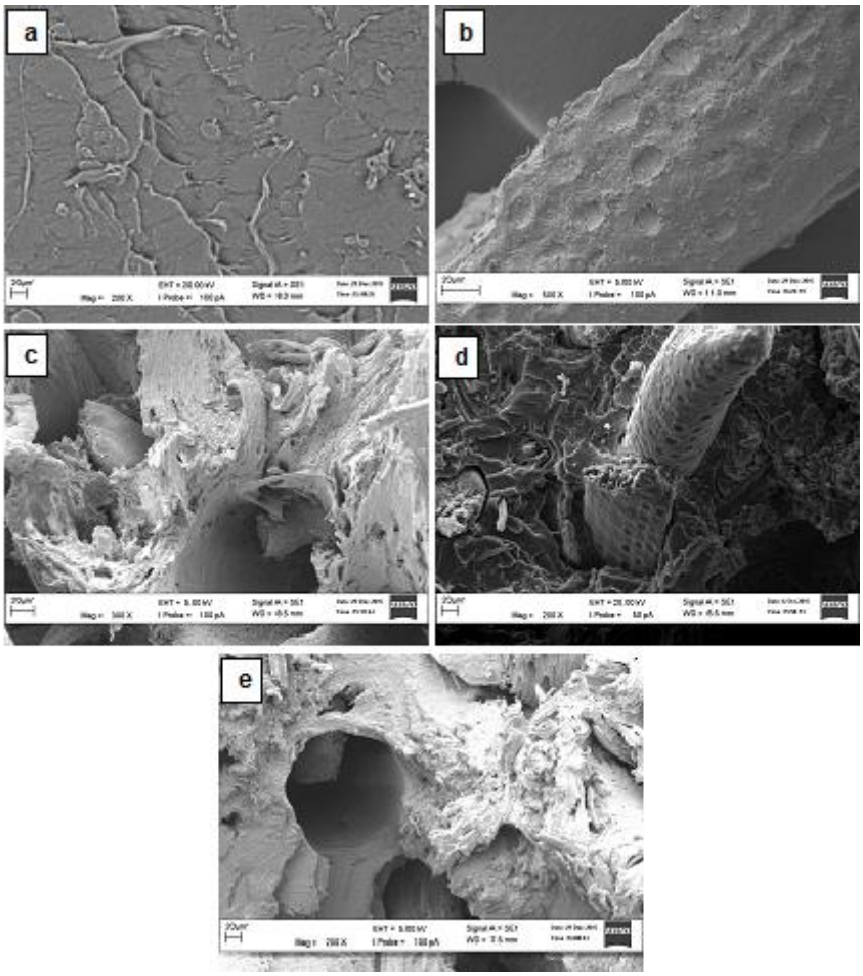

Fig. 9. SEM of (a) pure TPU, (b) SPF, (c) 160 µm TPU-SPF, (d) 250 µm TPU-SPF, and (e) 425 µm TPU-SPF

TGA

The thermogravimetric analysis is used to measure the mass change, thermal decomposition, and thermal stability of composite materials (Kim *et al.* 2004). Figure 10 demonstrates the TGA curves for the pure TPU and TPU-SPF composites. The residual mass percentage of the TPU and respective fiber sizes are demonstrated in Table 3. For all formulations, a slight mass loss was observed below 100 °C, which was attributed to the evaporation of absorbed moisture.

The composites 250 µm TPU-SPF (428 °C) and 425 µm TPU-SPF (425 °C) decomposed at a slightly higher temperature than 160 µm TPU-SPF (417 °C), indicating that the interaction between the fiber and matrix increased with the increasing fiber size. All SPF composites decomposed at a temperature lower than the pure TPU (431°C), indicating a lower interaction between the fiber and matrix (Alvarez *et al.* 2006; El-Shekeil *et al.* 2012).

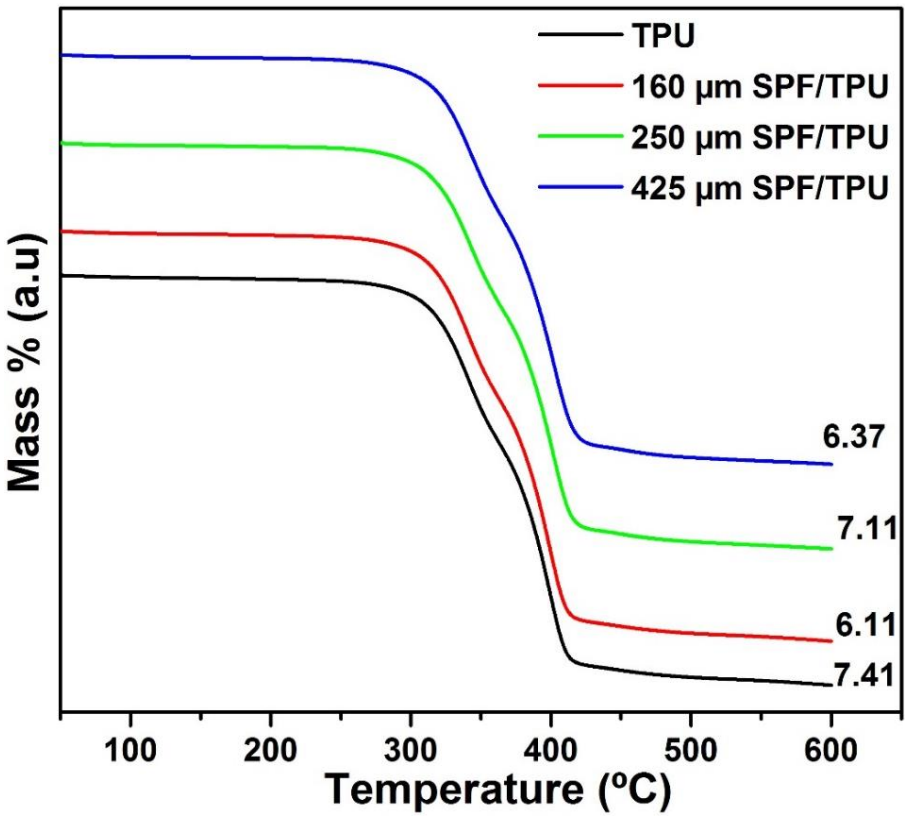

Fig. 10. TGA of pure TPU and TPU-SPF composites

Table 3. Residual Mass Percentage of Pure TPU and TPU-SPF Composites

Samples	Residual Mass (%)		
	$T_{26.99}$ (°C)	$T_{303.00}$ (°C)	$T_{599.16}$ (°C)
Pure TPU	99.69	94.18	7.41
160 µm TPU-SPF	99.65	94.30	6.11
250 µm TPU-SPF	99.73	94.46	7.11
425 µm TPU-SPF	99.76	94.76	6.37

CONCLUSION

The development of environmentally friendly composite of the TPU-SPF was successfully achieved, and process conditions were optimized accordingly. The

physicochemical studies confirmed the best-optimized condition for preparation, such as 40 rpm rotational velocity; temperature ~ 190 °C; ~ and size of 250 µm, respectively, to achieve the best possible tensile strength value of ~14 MPa.

ACKNOWLEDGMENTS

This work was supported financially by the Ministry of Higher Education (MOHE) of Malaysia and the University Malaysia Pahang (UMP) through the Fundamental Research Grant Scheme (RDU130138) and Graduate Research Scheme (GRS1503124), respectively. Moreover, the authors are thankful to University of Technology, Baghdad, Iraq, for all supports.

REFERENCES CITED

Aji, I. S., Zainudin, E. S., Khalina, A., Sapuan, S., and Khairul, M. (2011). "Studying the effect of fiber size and fiber loading on the mechanical properties of hybridized kenaf/PALF-reinforced HDPE composite," *Journal of Reinforced Plastics and Composites* 30(6), 546-553. DOI: 10.1177/0731684411399141

Alvarez, V., Rodriguez, E., and Vázquez, A. (2006). "Thermal degradation and decomposition of jute/vinylester composites," *Journal of Thermal Analysis and Calorimetry* 85(2), 383-389. DOI:10.1007/s10973-005-7102-0

ASTM D256-10e (2010), "Standard test methods for determining the Izod pendulum impact resistance of plastics," ASTM International, West Conshohocken, USA.

ASTM D638-02a (2002), "Standard test method for tensile properties of plastics," ASTM International, West Conshohocken, USA.

ASTM D790-03 (2003), "Standard test methods for flexural properties of unreinforced and reinforced plastics and electrical insulating materials," ASTM International, West Conshohocken, USA.

Bachtiar, D., Salit, M. S., Zainuddin, E., Abdan, K., and Dahlan, K. Z. H. M. (2011). "Effects of alkaline treatment and a compatibilizing agent on tensile properties of sugar palm fiber-reinforced high impact polystyrene composites," *BioResources* 6(4), 4815-4823. DOI:10.1088/1757-899X/11/1/012012

Bachtiar, D., Sapuan, S. M., and Hamdan, M. M. (2008). "The effect of alkaline treatment on tensile properties of sugar palm fiber reinforced epoxy composites," *Materials & Design* 29(7), 1285-1290. 012012. DOI:10.1016/j.matdes.2007.09.006

Bachtiar, D., Sapuan, S., and Hamdan, M. M. (2009). "The influence of alkaline surface fiber treatment on the impact properties of sugar palm fiber-reinforced epoxy composites," *Polymer-Plastics Technology and Engineering* 48(4), 379-383. DOI:10.1080/03602550902725373

Bachtiar, D., Sapuan, S. M., and Hamdan, M. M. (2010). "Flexural properties of alkaline treated sugar palm fiber reinforced epoxy composites," *International Journal of Automotive and Mechanical Engineering (IJAME)* 1, 79-90. DOI:10.15282/ijame.1.2010.7.0007

Bachtiar, D., Sapuan, S. M., Khalina, A., Zainudin, E., and Dahlan, K. (2012). "Flexural and impact properties of chemically treated sugar palm fiber reinforced high impact

polystyrene composites," *Fibers and Polymers* 13(7), 894-898. DOI:10.1007/s12221-012-0894-1

Bachtiar, D., Sapuan, S. M., Khalina, A., Zainudin, E. S., and Dahlan, K. (2010). "The tensile properties of single sugar palm (*Arenga pinnata*) fiber," *IOP Conference Series: Materials Science and Engineering*. 11. 012012. DOI:10.1088/1757-899X/11/1/012012

Biagiotti, J., Puglia, D., and Kenny, J. M. (2004). "A review on natural fiber-based composites-part I: structure, processing and properties of vegetable fibers," *Journal of Natural Fibers* 1(2), 37-68. DOI:10.1300/J395v01n02_04

Bos, H. L., Müssig, J., and van den Oever, M. J. (2006). "Mechanical properties of short-flax-fiber reinforced compounds," *Composites Part A: Applied Science and Manufacturing* 37(10), 1591-1604. DOI:10.1016/j.compositesa.2005.10.011

Caulfield, D. F., Jacobson, R. E., Sears, K. D., and Underwood, J. H. (2001). "Wood pulp fibers as reinforcements for high-melting engineering thermoplastics for 'under-the-hood' automotive applications," in: Conference proceedings of the Polymer Processing Society 17th annual meeting; May 21-24; Montreal, Canada. 10.

Dittenber, D. B., and GangaRao, H. V. S. (2012). "Critical review of recent publications on use of natural composites in infrastructure," *Composites Part A: Applied Science and Manufacturing* 43(8), 1419-1429. DOI:10.1016/j.compositesa.2011.11.019

El-Shekeil, Y. A., Salit, M. S., Abdan, K., and Zainudin, E. S. (2011). "Development of a new kenaf bast fiber-reinforced thermoplastic polyurethane composite," *BioResources* 6(4), 4662-4672.

El-Shekeil, Y., Sapuan, S., Abdan, K., and Zainudin, E. (2012a). "Influence of fiber content on the mechanical and thermal properties of Kenaf fiber reinforced thermoplastic polyurethane composites," *Materials & Design* 40, 299-303. DOI:10.1016/j.matdes.2012.04.003

El-Shekeil, Y., Sapuan, S., Khalina, A., Zainudin, E., and Al-Shuja'a, O. (2012b). "Effect of alkali treatment on mechanical and thermal properties of kenaf fiber-reinforced thermoplastic polyurethane composite," *Journal of Thermal Analysis and Calorimetry* 109(3), 1435-1443. DOI:10.1007/s10973-012-2258-x

El-Shekeil, Y. A., Sapuan, S., and Algrafi, M. W. (2014). "Effect of fiber loading on mechanical and morphological properties of cocoa pod husk fibers reinforced thermoplastic polyurethane composites," *Materials & Design* 64, 330-333. DOI:10.1016/j.matdes.2014.07.034

Engels, H. W., Pirkl, H. G., Albers, R., Albach, R. W., Krause, J., Hoffmann, A., Casselmann, H., and Dormish, J. (2013). "Polyurethanes: Versatile materials and sustainable problem solvers for today's challenges," *Angewandte Chemie International Edition* 52(36), 9422-9441. DOI: 10.1002/anie.201302766

Gunatillake, P., Mayadunne, R., and Adhikari, R. (2006). "Recent developments in biodegradable synthetic polymers," *Biotechnology Annual Review* 12, 301-347. DOI:10.1016/S1387-2656(06)12009-8

Herrera, M., Matuschek, G., and Kettrup, A. (2002). "Thermal degradation of thermoplastic polyurethane elastomers (TPU) based on MDI," *Polymer Degradation and Stability* 78(2), 323-331. DOI:10.1016/S0141-3910(02)00181-7

Ishak, M., Sapuan, S., Leman, Z., Rahman, M., Anwar, U., and Siregar, J. (2013). "Sugar palm (*Arenga pinnata*): Its fibers, polymers and composites," *Carbohydrate Polymers* 91(2), 699-710. DOI:10.1016/j.carbpol.2012.07.073

Jawaid, M., and Khalil, H. A. (2011). "Cellulosic/synthetic fiber reinforced polymer hybrid composites: A review," *Carbohydrate Polymers* 86(1), 1-18. DOI:10.1016/j.carbpol.2011.04.043

Kanimozhi, K., Sethuraman, K., Selvaraj, V., and Alagar, M. (2014). "Development of ricehusk ash reinforced bismaleimide toughened epoxy nanocomposites," *Frontiers in Chemistry* 2. DOI:10.3389/fchem.2014.00065

Kim, H.-S., Yang, H.-S., Kim, H.-J., and Park, H.-J. (2004). "Thermogravimetric analysis of rice husk flour filled thermoplastic polymer composites," *Journal of Thermal Analysis and Calorimetry* 76(2), 395-404. DOI:10.1023/B:JTAN.0000028020.02657.9b

Kim, Y., Kwon, O. H., Park, W. H., and Cho, D. (2013). "Thermomechanical and flexural properties of chopped silk fiber-reinforced poly (butylene succinate) green composites: effect of electron beam treatment of worm silk," *Advanced Composite Materials* 22(6), 437-449. DOI:10.1080/09243046.2013.843830

Liang, J.-Z. (2012). "Predictions of Young's modulus of short inorganic fiber reinforced polymer composites," *Composites Part B: Engineering* 43(4), 1763-1766. DOI:10.1016/j.compositesb.2012.01.010

Liang, J. and Li, R. (1998). "Mechanical properties and morphology of glass bead–filled polypropylene composites," *Polymer Composites* 19(6), 698-703. DOI:10.1002/pc.10142

Liang, J., Li, R., and Tjong, S. (1999). "Tensile properties and morphology of PP/EPDM/glass bead ternary composites," *Polymer Composites* 20(3), 413-422. DOI:10.1002/pc.10367

Matheson, T. (2009). "*Impact of Dispersion of Interfaces on the Rheology of Polymeric Nanocomposites*," Master thesis, University of Southampton, UK.

Misra, M., Mohanty, A., Tummala, P., and Drzal, L. (2004). "Injection molded biocomposites from natural fibers and modified polyamide," in: *ANTEC Conference Proceedings*, Chicago, USA, Vol. 2, pp. 1603-1607).

Özgür Seydibeyoğlu, M., and Oksman, K. (2008). "Novel nanocomposites based on polyurethane and micro fibrillated cellulose," *Composites Science and Technology* 68(3-4), 908-914.

Pilla, S. (ed.) (2011). *Handbook of Bioplastics and Biocomposites Engineering Applications*, John Wiley & Sons, Massachusetts, USA.

Ratnam, C. T., Fazlina, R. S., and Shamsuddin, S. (2010). "Mechanical properties of rubber-wood fiber filled PVC/ENR blend," *Malaysian Polymer Journal* 5(1), 17-25.

Roy, A., Chakraborty, S., Kundu, S. P., Basak, R. K., Majumder, S. B., and Adhikari, B. (2012). "Improvement in mechanical properties of jute fibers through mild alkali treatment as demonstrated by utilisation of the Weibull distribution model," *BioResource Technology* 107, 222-228. DOI:10.1016/j.biortech.2011.11.073

Vera-Sorroche, J., Kelly, A., Brown, E., Coates, P., Karnachi, N., Harkin-Jones, E., Li, K., and Deng, J. (2013). "Thermal optimisation of polymer extrusion using in-process monitoring techniques," *Applied Thermal Engineering* 53(2), 405-413. DOI:10.1016/j.applthermaleng.2012.04.013

Verhoeven, V. W. A. (2006). "The reactive extrusion of thermoplastic polyurethane," PhD thesis, University of Groningen, Netherland.

Wötzel, K., Wirth, R., and Flake, M. (1999). "Life cycle studies on hemp fiber reinforced components and ABS for automotive parts," *Die Angewandte Makromolekulare Chemie* 272(1), 121-127. DOI: 10.1002/(SICI)1522- 505(19991201)272:1<121::AID-APMC121>3.0.CO;2-T

Article submitted: April 15, 2016; Peer review completed: June 17, 2016; Revised version received: September 11, 2016; Accepted: September 12, 2016; Published: September 21, 2016.
DOI: 10.15376/biores.11.4.9438-9454